Diagnosis of Covid-19 using Fractional B-spline Wavelet Transform in Lung Ultrasound images

Salar Mohammadi [a], Saeid Rashidi [a*]

[a] Department of Biomedical Engineering, College of Medical Science and Technologies, Tehran Science and Research Branch, Islamic Azad University, Tehran, Iran.

First Author:

Salar Mohammadi, MSc
Department of Biomedical Engineering, College of Medical Science and Technologies, Tehran Science and Research Branch, Islamic Azad University, Tehran, Iran.
Tel: (+98)9126451400
G-mail: Salar.moh.bme@gmail.com

***Corresponding Author:**

Saeid Rashidi, PhD
Department of Biomedical Engineering, College of Medical Science and Technologies, Tehran Science and Research Branch, Islamic Azad University, Tehran, Iran.
Tel: (+98) 912 434 0786
G-mail: rashidi.saeid@gmail.com

Abstract

The coronavirus spread rapidly in the world and caused the disease of Covid-19. The proposed research was conducted with the aim of classifying people with Covid-19 from other people. lung ultrasound images were used to diagnose covid-19. The open source Point-Care-of-Ultrasound (POCUS) database was collected, which contained 59 Lung Ultrasound (LUS) images and was collected from several other databases. In this research, KNN classifier with K-fold cross validation was used to classify the feature matrix obtained from Fractional B-spline Wavelet Transform (FBSWT). The proposed method, Block-Matching and 3D filtering (BM3D) filter was used in some methods, which had acceptable results. The proposed method was used to classify healthy people from patients with Covid-19. The results show that when the features based on the wavelet transform (WT) are used, the proposed method can be achieved 90.90% sensitivity, 92.30% specificity, and 91.42% accuracy. While the features extracted from FBSWT show that the proposed method can be achieved 95.45% sensitivity, 93.30% specificity, and 94.28% accuracy. Fractional transforms, especially the FBSWT, can be a useful tool for image processing. They can be used for various purposes such as detection and classification. By using FBSWT, it is possible to accurately diagnose the disease of covid-19.

Keywords: Fractional Wavelet Transform, B-spline, Ultrasound, Covid-19, BM3D Filtering

1. Introduction

Acute respiratory syndrome coronavirus 2 is an enveloped positive-sense genomic single-stranded ribonucleic acid (RNA) virus that causes coronavirus disease 2019 (COVID-19) and is contagious to humans and is transmitted through close human interactions or the spread of respiratory secretions such as coughs and sneezes [1]. This respiratory disease caused by the novel coronavirus 2019 is detected by a nucleic acid amplification test, Attempts should be made to use saliva samples for the diagnosis of COVID-19 to reduce the risk of infection of medical personnel [2]. In humans, various viruses are asymptomatic or accompanied by fever, cough, shortness of breath, and gastrointestinal irritation [3].

Pneumonia is a common acute respiratory infection involving the alveoli and distal airways. It is a major health problem and is associated with great morbidity and short-term and long-term mortality in all age groups worldwide [4]. Due to cardiopulmonary disease or patient's defense deficiency, pneumonia in elderly patients is associated with increased mortality and complications compared to people. The clinical importance of pneumonia in the elderly is related to age-related and pathological changes in the immune system as well as the lungs [5].

In this research, LUS images have been used to detect damaged lung tissue. Using these images has the advantages of being painless and non-invasive, easy when using an ultrasound device, this type of imaging method has a lower cost than other imaging methods such as computed tomography (CT) and Magnetic Resonance Imaging (MRI). One of the main advantages of ultrasound imaging is the absence of x-ray radiation to the patient. Lung ultrasound is a suitable method to diagnose lung diseases.
The image quality is sufficient, appropriate and the sound window of the lung is always recorded. Ultrasound imaging is less than 1 minute for 2 objectives, targeting pleural fluid (pleural effusion) and lung fluid (pulmonary congestion as multiple B-lines) [6]. Ultrasound imaging of the lung and associated tissues may play an essential role in the management of patients with lung injury associated with COVID-19. Compared with other monitoring methods, such as auscultation or radiographic imaging, it is argued that LUS has higher diagnostic accuracy, is ergonomically favorable, and has limited control implications [7].

In the proposed study, with the help of different classifications and the use of Artificial Intelligence (AI), the healthy group of patients has been diagnosed. Artificial intelligence is a general term that refers to the use of computers to model intelligent behavior with minimal human intervention [8]. Artificial intelligence techniques can be an effective tool to combat the pandemic caused by COVID-19. In the review paper by Kumar et. al, various artificial intelligence-based techniques for the prediction and diagnosis of the disease of COVID-19 are studied and evaluated. AI-based predictive models can be used to predict mortality, infection in patients through cough and biomarkers, genome structure associated with mortality, and severity. Artificial intelligence has the potential to screen populations and predict risk. In Kumar's study, additional explanations regarding the diagnosis and treatment of Covid-19 patients based on artificial intelligence are evaluated [9].

The progression of the disease of Covid-19 in a person's lung is shown from left to right in figure 1. A lines that exist horizontally in the lung indicate a healthy lung. Afterwards, the corona virus imposes the body, the lungs enter the moderate stage of the disease. As the condition becomes acute, lines A are gradually eliminated and vertical lines B appear, which indicates the increase of the disease. Advanced in this case, this disease is in the critical stage where the lung infection does not follow a specific pattern and the infection spreads sporadically in the lung. In the proposed research, mathematical transforms of the WT and FBSWT were applied on the ultrasound images of the studied subjects and then useful statistical features were extracted from the lung images of the subjects and after forming the feature matrix with the help of classifiers, they were classified images are paid.

The WT provides high frequency resolution at lower frequencies while degrading the resolution at higher frequencies. Therefore, the WT is a multi-resolution tool. Low resolution represents an approximation and higher resolution represents fine detail of a signal. Each time the WT is applied, a low resolution signal (low frequency L) and a fine detail signal (high frequency H) are obtained, both They are half the size of the original signal [10]. The WT increases the noise ratio of images peak signal-to-noise ratio (PSNR) [11].

Fractional Wavelet Transform (FWT) also means performing a Fractional Fourier Transform (FFT) with optimal fractional order *p* on the entire input view and then performing wavelet analysis [12]. A new Fractional Wavelet Transform (FRWT) is proposed to modify the WT and Fractional Fourier Transform (FRFT) configurations. The proposed transform not only inherits the multi-resolution analysis of the WT but also can display in the fractional domain, which is similar to the FFT. The novel fractional wavelet transform can provide representation in the fractional time-frequency domain [13]. The FBSWT also used in this study due to the smaller computational volume.

In this study, a time-frequency transform called FBSWT was used to extract features, which has a high speed and creates real coefficients.

The rest of the paper is organized as follows: In part 2, the proposed method and materials were discussed, which includes the description of the database, feature extraction. Section 3 includes results and classification. Section 4 discussed and compared the proposed work with other methods, and section 5 concluded.

1.1 Related works

Diagnosing pulmonary pathologies with the help of machine learning from lung ultrasound images is a relatively new field of research. Ultrasound can indicates thickening of the pleural line and other physiological phenomena associated with changes in lung structure when the infection is in the early stages. Studies report abnormalities in B-lines as well as detectable lesions in the lower lobes of the lung as key features for the diagnosis of COVID-19. In the rest of this section, the past literature will be introduced in order to diagnose and classify people with covid-19 from other ultrasound images.

Muhammad et. al proposed a convolutional neural network (CNN) model that has fewer learning parameters but can achieve high accuracy. This model has five main blocks or layers of twist connectors. A multi-layer hybrid function of each block is proposed to improve the efficiency of the screening method for COVID-19 using the proposed model. Experiments are performed using freely available LUS images. The proposed fusion method has 92.5% precision, 91.8% accuracy, and 93.2% retrieval using data collection. These levels of efficiency metrics are significantly higher than those used in any of the advanced versions of CNN [14].

In another study, Born et. al advocate a more prominent role for point-of-care ultrasound imaging to guide the diagnosis of COVID-19. The data of this work from open source databases was collected. A deep convolutional neural network (VID-Net) was trained on this three-classes dataset and achieved 89% accuracy, 96% Sensitivity, and 79% specificity [15].

Olgerz et. al proposed core LUS competencies for internists that may be included in internal medicine training requirements in Europe. Olgerz suggests using a competency-based training system of Trusted Professional Activities (EPA) with EPAs specifically designed for ultrasound [16].

Deep convolutional neural networks have emerged as a powerful tool to provide successful performance in the analysis and processing of various images. However, DCNNs are without a strong theoretical foundation and require a large amount of training data. Jun Shi et. al aim to overcome these drawbacks by using a FWT, which can be viewed as a bank of linearly varying multiband filters, and may be suitable for non-stationary texture analysis [17].

Diaz-Escobar tested various pre-trained deep learning architectures, including VGG19, InceptionV3, Xception, and ResNet50, on his database. The database used in Diaz-Escobar study is POCUS. Predictive models were used considering three classes (COVID-19, pneumonia, and healthy) and two classes (COVID-19 vs. pneumonia and COVID-19 vs. non-COVID-19). To evaluate the performance, classification criteria of each class (accuracy, recall, and F1 score) and overall criteria (accuracy and area under the receiver operating characteristic curve) were calculated. Finally, a statistical analysis of performance results was performed using ANOVA and Friedman tests, followed by post hoc analysis using the Wilcoxon signed rank test. The InceptionV3 network achieved the best average accuracy (89.1%) and area under the receiver operating curve (97.1%) for detecting COVID-19 from bacterial pneumonia and healthy lung ultrasound data [18].

Ebadi et. al proposed a method for fast and reliable interpretation of lung ultrasound images using learning, based on the Kinetics-I3D network. The learned model can use the entire lung ultrasound scan obtained from the point of care to classify without the need for preprocessing or frame-by-frame analysis. Annotated video classifiers provided by sets of radiologists and specialist physicians are compared, including A-lines, B-lines, stabilization, and pleural effusion. The classification method using 5-fold cross-validation reaches 90% accuracy and an average accuracy score of 95% [19].

Baum et al. presented a novel two-step computer-aided system for lung abnormality detection using lung ultrasound imaging for the diagnosis of covid-19 disease. This system uses a combination of two deep learning models. In this study, 37 patients

with covid-19 and 12 people whose disease was controlled were evaluated. One module improves the quality of images and another module diagnoses the disease. The average classification accuracy, sensitivity and specificity in detecting positive cases of Covid-19 were 95%, 91% and 97%, respectively. The integration of these two modules provides accurate, rapid and practical diagnostic guidance and assistance for patients with suspected respiratory conditions at the point of care [21].

Awasthi et. al developed an efficient lightweight mobile-friendly deep learning model for the diagnosis of COVID-19 using lung ultrasound images. The data of this study were divided into three different classes including COVID-19, pneumonia, and healthy. The developed Mini-COVIDNet network was used as the title network and evaluated with other neural network models with advanced heavy models. The results showed that the proposed network can achieve the highest accuracy of 83.2% and requires only 24 minutes of training time. The proposed Mini COVIDNet has 4.39 times fewer parameters compared to its next best network and requires only 51.29 MB of memory, which makes accurate diagnosis of COVID-19 using lung ultrasound imaging feasible on a mobile phone [21].

2. Material and Methods

The overview of the proposed scheme is shown in Figure 2 that shows four methods have been investigated.

I: Using WT without BM3D filter.

II: Using WT with BM3D filter.

III: Using FBSWT without BM3D filter.

IV: Using FBSWT with BM3D filter.

In method I, the WT was used to apply the Haar function obtained from trial and error. The WT was used in case II and first it was applied to the images of the proposed BM3D filter and then the initial coefficients were extracted using WT. Then the coefficients were used to reduce the dimensions and finally the classification work was done. After applying this transform, because the images are not the same size, it was decided to proceed with two levels of the WT analysis. After applying the WT to the images, four categories of total coefficients are obtained: approximation, vertical, horizontal, and detail coefficients. This method used the coefficients of the second level of analysis and the set of vertical coefficients. The reason for using these coefficients was the presence of vertical lines B in the patient's ultrasound images, which are selected by choosing this set of coefficients of the vertical frequencies of the image. Finally, the first high-volume feature matrix is formed.

In the case of III, FBSWT is applied to the images without applying BM3D filter. It should be noted that in this case and the next case that is expressed, the information is one-dimensional as the output of the transform. Since the degree of freedom is one of the essential parameters under investigation, it was investigated between -0.5 and 1. The best alphas in each section were obtained from trial and error. In this case, a feature matrix equal to the number of samples is obtained.

In the case of IV, all the conditions are the same as in case b, with the difference that first, the images are used from the proposed BM3D filter. Finally, a one-dimensional feature matrix is obtained as in the previous method. Now four feature matrices with high volume are available. For each feature, reduction and extraction of secondary features must be applied. These features are obtained from statistics that include Kurtosis, Skewness, Standard Deviation, Variance, Entropy, Average, Maximum and Minimum coefficients.

Finally, features set were evaluated by KNN classification with the K-Fold cross validation and N=10. The results of the four criteria of F1-score, sensitivity, specificity, and accuracy are generally expressed.

2.1. Database

The data includes more than 200 videos and more than 60 images from 3 classes (Covid-19, pneumonia, healthy lungs). From the machine learning community, unlike computer tomography and X-Ray imaging, ultrasound has not yet attracted much attention in the field of Covid-19. However, many in the medical community favor a more prominent role for ultrasound in the current pandemic [22]. Figure 3 shows the images of three classes of Covid-19, pneumonia and healthy lung in ultrasound images.

This research has created a collection of LUS images and videos. This data set is collected from financial donations of hospitals as well as public resources available on the web (mainly publications and educational websites). 162 films include 49 films on Covid-19, 49 films on bacterial pneumonia, 64 films on health, and 3 films on viral pneumonia. 20 movies from the Butterfly dataset, 18 Covid-19 movies, 2 healthy movies. 53 images include 18 images of Covid-19, 20 images of bacterial pneumonia and 15 healthy images.

In this database, 20 videos include 6 videos of Covid-19, 2 videos of bacterial pneumonia, 9 videos of healthy pneumonia, and 3 videos of viral pneumonia. 6 images include 4 images of Covid-19 and 2 images of bacterial pneumonia. 45 videos of possible Covid-19 patients have been collected in Piacenza at the height of the crisis in Italy. The PCR test was not sufficient, so the label is not clear. For more information and comments from medical professionals, visit the CSV Metadata page.

This database provides the largest publicly available pre-processed lung POCUS dataset, which includes a sample of covid-19 patients, pneumonia-infected lungs, and healthy patients. As shown in Table 1, this database contains 139 recordings (106 videos + 33 images) recorded with convex or linear probes, where the latter is a higher frequency probe and Provides more surface images. All samples from the database mentioned are annotated and verified by a physician. Additionally, notes have been added about visible patterns in each video (Eg B-Lines or blends). 59 images were used in this work.

The supplementary information of the database includes the severity of the disease from 0 to 3, physicians' opinions, frame rate, resolution, frame length and binary symptoms such as cough, fever and headache. The gender of the patients has also been discussed, but there is no information about the gender of all the patients.

2.2. Pre-processing

Speckle noise is a type of noise that affects the nature of the medical ultrasound image. The effectiveness of this process can be improved by removing noise without affecting essential image features [23]. Here it discusses in detail the categories of main filter to reduce noise in images. Then feature extraction with the classical transform method, the proposed filter, is used to improve the performance of the designed classification methods. In other methods, images are used without proposed filter. It should be noted that the results are expressed in two ways. A filter has been applied to some images, a FWT has been applied, and finally, features have been extracted. No filter was applied to some images, and WT and FBSWT were applied to the raw images; then feature was extracted.

Image noise is an unwanted factor that, in addition to having an adverse effect on image quality, also complicates processes such as compression, edge detection, and image segmentation. Most of the latest filters for filtering speckle noise do not consider the shape of objects (to certain edges) in images and even destroy the essence and original information of the image. Block matching and three-dimensional filtering were discussed in order to modify the output of intermediate techniques on decision and matching. The obtained results are excellent and surpass the current situation by about 2 dB for color and grayscale images [23]. Block matching and three-dimensional filtering can improve filtering around edges, objects and other details by looking for similar patches and duplicate details [24]. However, there is still a lot of room for improvement in this algorithm to achieve more attractive results [25]. Figure 4 indicates the structure of the proposed Block matching and three-dimensional filter in general.

In filtering, the purpose of using a filter is to preserve the valuable information of the image. Figure 5 shows the LUS image before and after applying the filter. Generally, the higher the signal-to-noise ratio, the more information is available from the image.

2.3. Wavelet Transform

Wavelet Coefficients Expands the concept of Fourier coefficients, a convolutional WT that measures the similarity between a wavelet function and a signal. The WT, which has become increasingly important in signal and image processing, includes possible implementations of new developments in image compression, image transmission, transient signal processing, and more [12]. The WT plays a fundamental role in processing unstable signals. Fourier transform does not provide any information about time (it has a high resolution in the frequency domain but zero in the time domain), Formula (1) shows the WT [27]:

$$W_x(a,b) = x(t) * \left(a^{-\frac{1}{2}} \varphi * \left(-\frac{t}{a} \right) \right) \quad (1)$$

Which φ is the continuous mother wavelet scaled by factor a and shifted by factor b. The value of the scaling factor and displacement are serial numbers. Figure 6 shows the decomposition of the image into two decomposition levels, and in this study, the images are divided into two decomposition levels in the WT.

2.4. Fractional B-spline Wavelet Transform

First, it should be known that the generalized fractional transform is a WT. This transform is similar to the WT in both time and frequency domains. However, due to the complexity of the calculations and the fact that computer systems can calculate a large amount of information, it is recommended to use a fractional wavelet of the B-spline type. The FWT has different definitions, one of these definitions is to use Fourier transform fraction and combine it with normal WT. The FWT has different definitions, one of these definitions is the use of fractional Fourier transform and its combination with WT. These new functions are local versions of one-way power functions [29]:

$$\beta_+^{\alpha} \overset{def}{=} \frac{\Delta_+^{\alpha+1} x_+^{\alpha}}{\tau(\alpha+1)} = \sum_{k \geq 0} \frac{(-1)^{k \binom{\alpha+1}{k}}}{\tau(\alpha+1)} (x-k)_+^{\alpha} \quad (2)$$

Where $\alpha > \frac{-1}{2}$ interpolates common polynomials to ensure the square integrity of these B-splines functions. As it is clear from formula (2), this is the causal formula of the FBSWT, which only covers positive alphas. By generalizing this formula, the symmetric mode of FBSWT is obtained, which covers negative degrees in addition to positive degrees of alpha. Formula (3) is a generalized state which consists of:

$$\beta_+^{\alpha} \overset{def}{=} \frac{\Delta_+^{\alpha+1} x_*^{\alpha}}{2\sin(\frac{\pi}{2}\alpha)\tau(\alpha+1)} = \sum_{k \in z} \frac{(-1)^{k+1 \binom{\alpha+1}{k}}}{2\sin(\frac{\pi}{2}\alpha)\tau(\alpha+1)} [x-k)^{\alpha} \quad (3)$$

Here, it is assumed that the factorial is extended to x by the integer $x! = T(x+1)$ using the Euler step function. As it turns out, this FWT can change the resolution by holding the alpha parameter. As it turns out, this FWT can change the resolution by holding the alpha parameter. The generalized FWT is a WT. By having an alpha degree, there is more practical freedom than a WT, which causes a different value to be given to the time and frequency domains simultaneously.

The FBSWT can be normalized if a standard method is used. The obtained functions satisfy the two-scale relation with the following filters, Formulas (4) and (5) show the filters obtained from orthonormal:

$$H_{\perp}^{\alpha}(e^{j\omega}) = H^{\alpha}(e^{j\omega})\sqrt{\frac{A^{2\alpha+1}(e^{j\omega})}{A^{2\alpha+1}(e^{2j\omega})}} \tag{4}$$

$$A^{\alpha}(e^{jw}) = \sum_{n\in Z} e^{-jn\omega}\int \beta_{+}^{\alpha}(x)\beta_{+}^{\alpha}(x+n)dx \tag{5}$$

Where $A^{\alpha}(Z)$ is the autocorrelation filter of B-spline of degree α. the wavelets themselves are constructed by a linear combination of scaled functions. In orthogonal mode, the filter has a frequency response in the following formula (6):

$$G_{\perp}^{\alpha}(e^{i\omega}) = e^{-j\omega}H_{\perp}^{\alpha}(-e^{-j\omega}) \tag{6}$$

In the orthogonal case, the frequency response of the generating filter is $G_{\perp}^{\alpha}$ and $H_{\perp}^{\alpha}$ satisfies a two-scale relation with conventional filters. In a way, $H_{\perp}^{\alpha}$ and $G_{\perp}^{\alpha}$ can be considered as filter banks of analysis and synthesis, respectively. According to the theory stated in formula (5), fractional spline wavelets have a fractional differentiation of order $\alpha+1$ for low frequencies. Where N is decomposition levels, N has to be a power of 2 and this equation, ω tends to 0. The reconstruction of X_n from Y_n and Z_n are shown in formula (7):

$$\begin{aligned} X_k &= \overline{H_{\perp k}^{\alpha}}Y_k + \overline{G_{\perp k}^{\alpha}}Z_k \\ X_{k+\frac{N}{2}} &= \overline{H_{\perp k+\frac{N}{2}}^{\alpha}}Y_k + \overline{G_{\perp k+\frac{N}{2}}^{\alpha}}Z_k \end{aligned} \tag{7}$$

It is assumed that the input signal by its coefficients $\{x_k\}k = 0 \ldots . N-1.$ This signal was expanded to any value of the index $k \in Z$ by periodization, i.e., $x_{N+k} \cong x_k$ .The reconstruction of X_k from Y_k and Z_k by the classical filter bank follows formula (6), since the filters are canonical. The proposed algorithm used follows the synthesis formula and it is obvious that each iteration of synthesis costs as much as one iteration of analysis.

The WT has some challenges which are:

- Choosing the right mother function
- Determining the optimal decomposition level

While in the WFT, knowing the appropriate alpha degree, usually obtained from trial and error, can be used more effectively in image processing. Considering that the volume of FWT calculations is complex and time-consuming, a particular type of FWT named B-spline was introduced, which has good speed and accuracy.

2.5. Feature Extraction

In the first proposed method, a WT is first applied to LUS images to form the initial feature matrix and the sum of the coefficients is obtained. The set of coefficients used is V2, as seen in Figure 7(A). Currently, the FBSWT is applied to the LUS images, and the feature matrix is obtained as one-dimensional information, as seen in figure 7(B). Now there are 2 primary feature matrices with large volume, one is the result of the WT, and the other is the result of the FBSWT. In the FBSWT, the information is converted into one dimension; to reduce the number of calculations, the matrix of coefficients in this transform is placed once in rows and once in columns. By trial and error, it was determined that the results in row mode are better than in column mode.

In order to reduce the features obtained from the two matrices of the previous step, the statistical formulas of skewness, kurtosis, mean, entropy, maximum and minimum coefficients, variance and standard deviation were used. Then, these features are used as input to the KNN classifier for classification. In this research, new coefficients were extracted from LUS images using WT and FWT based on B-spline. Also, by performing statistical operations applied to the coefficients of the

LUS images, several secondary statistical features were obtained from each matrix of coefficients. These features are fully explained. Now, to compare and analyze the results, some experimental criteria were used. In this study, KNN classification was used with K-fold evaluation methods. In this work, the value of N=10 was considered. The experimental criteria for evaluating the machine learning proposed for classifying Covid-19 disease from healthy people included: sensitivity, accuracy, specificity, and F1-score. The evaluation criteria were used once for two groups of patients (pneumonia and Covid-19) and healthy people, and they were tested once only for two groups of healthy people and Covid-19.

3. Results

KNN classification is discussed in the results section with k-fold evaluation method with n=10. As it is clear from the results, KNN classifier with k-fold evaluation method has performed better in this section. To find the best distance in each method, the best distance, alpha, and neighborhood number were obtained by taking the average of all evaluation criteria and trial and error. K=1 had the best results in all analyzes and with increasing K value, the results were decreasing.

In predictive models, cross-validation techniques are used to estimate the degree of generalization of the classification algorithm to unknown data. A common approach to evaluate the performance of a classification model on a specific data set is k-fold cross-validation. Generally, this technique randomly divides the original data set into two different subsets, the training set: 1-1/N percent of the samples, and the test set: 1/N percent of the samples. This method is repeated K times and for each repetition, different subsets are selected. In this paper, four evaluation criteria including accuracy, sensitivity, specificity and F1-score were analyzed. The evaluation criteria of Specificity, Sensitivity, Accuracy and F1-score are shown in formulas (8), (9), (10) and (11) respectively:

$$Specificity = \frac{TN}{TN + FP} \tag{8}$$

$$Sensitivity = \frac{TP}{TN + FP} \tag{9}$$

$$Accuracy = \frac{TP + TN}{TP + FP + TN + FN} \tag{10}$$

$$F1 - score = 2 * \left[\frac{(\text{Re}call * Precision)}{\text{Re}call * Precision} \right] \tag{11}$$

True Positive (TP): A test result that correctly indicates the presence of a condition or specificity.

True Negative (TN): A test result that correctly indicates the absence of a condition or specificity.

False Positive (FP): A test result which wrongly indicates that a particular condition or attribute is present.

False Negative (FN): A test result which wrongly indicates that a particular condition or attribute is absent

The classification in this research is done in two ways, the first one includes the selection of people into two groups of healthy people and patients (Covid-19 and pneumonia) and the other two-class classification method that includes only healthy people and Covid-19. In the second case, people with pneumonia were excluded from the data. Figure 8 shows an overview of how to classify the studied classes:

According to Figure 9, the features used in the feature reduction stage were evaluated with sensitivity and specificity criteria. Acceptable results were obtained according to Figure 9. Each feature was tested by KNN classification and the K-Fold evaluation method. Choosing a suitable feature is always one of the main challenges. According to the extracted statistical features, the value and validity of each feature have been checked in Figures 9 and 10, respectively.

The figure 10 reveals the feature box plot is the statistical features used in the proposed research, some of the features obtained from the second stage of extraction to reduce the feature dimensions in terms of mean and quartile were checked with each other in terms of accuracy and sensitivity, which were standard deviation and kurtosis. respectively, they have the highest accuracy and sensitivity.

According to Figure 10, the normalized features were examined by the Z-Score method. The reason for the existence of negative values of the coefficients was obtained from the WT. In the following, the proposed WT algorithm will be evaluated using the proposed BM3D filter on the images and then without using the filter.

Figure 11 shows the results of using different distances in KNN classifier with WT. The obtained results were analyzed in four different cases. Two classes of healthy and patient (pneumonia and covid-19) were classified with the proposed BM3D filter and without filter. In the other case, the matrix of features obtained from healthy people and Covid-19 were classified once with the proposed filter of BM3D and again without using the filter.

The best distance in two classes, patient and healthy, using the BM3D filter in the WT is the correlation distance, but in the image without filter, in this case, the Mahalanobis distance is the best distance. In two classes, healthy and Covid-19, using the BM3D filter, Mahalanobis distance is the best distance, and if the correlation distance filter is not used, the distance is superior.

The results of the evaluation criteria measured in the classification, which include sensitivity, specificity, accuracy and F1 score in the WT method is showed in Table 2. With the gradual increase of K, the results of evaluation criteria are decreasing. These results were examined in two classes, healthy and patient.

Healthy and Covid-19 classes using WT is showed in table 3. The matrix of features obtained from lung ultrasound images was evaluated in two ways, by BM3D filter and without BM3D filter. As the value of K increases, the evaluation criteria decrease.

The distances were examined in FBSWT method is showed in figure 12. Similarly, the WT, this method was also studied in four conditions. The studied methods with FBSWT included healthy and patient groups (pneumonia and covid-19) as well as healthy and covid-19, and the results were expressed as filtered and unfiltered for each group. The value of alpha degree was obtained experimentally.

According to Figure 12, the best distance in both healthy and diseased groups is Mahalanobis distance by applying BM3D filter and correlation distance in images without filter. Also, in both healthy and Covid-19 classes, the best distance with BM3D filter and without filter is correlation and Euclidean distance, respectively. Table 4 shows the evaluation criteria in FBSWT in appropriate alphas.

The optimal alpha is 0.7 and 0.8 for two methods with BM3D filter and without filter, respectively, that shows in table 4. In the first case, when the filter was used, the best results of sensitivity, specificity, accuracy and F1 score were obtained from k=1.

Acceptable results were obtained from both healthy and Covid-19 groups with BM3D filter and without filter. The appropriate alpha in the mode of using the filter is 0.6 and in the mode without the filter, alpha is 0.8, the results of which can be seen in Table 5.

The confusion matrix of the best results for the two healthy and Covid-19 classes, using the BM3D filter, is shown in Figure 13. This result was obtained from Mahalanobis distance and k=1. In this section, only two healthy and Covid-19 classes were evaluated. The number of people with covid-19, 22 people and 13 healthy people were evaluated. Figure 13 shows the evaluation criteria of sensitivity, characteristic, accuracy and F1 score along with the standard deviation in the best case.

The classification results of different classes with BM3D filter and without filter are shown in Table 6. In the classification of two classes, healthy and Covid-19, FBSWT had better results compared to WT.

1. Discussion

Machine learning algorithms were able to predict with good performance the risk of each patient having a positive result for COVID-19. Our contribution to this track is exploring automated detection of COVID-19 by lung ultrasound imaging to provide a rapid assessment of a person's likelihood of contracting COVID-19. Our first step to achieve this goal was to use a set of POCUS database images collected and preprocessed from referenced sources.

The method of FBSWT is considered as an innovation, which is the predictive power of the data and also expresses the capabilities of a model to detect specific patterns in lung ultrasound data, the first it gives in them. slow Searching is done to develop digital tools that can be used for useful information from databases. The FWT is a generalized WT and the resolution can be checked in both time-frequency domains. The B-spline type is a FWT that has less computational volume and complexity compared to other mother features. The proposed algorithm in this study obtains coefficients from lung ultrasound images, which can show the difference between classes. Searching is done to develop digital tools that can be used for useful information from databases. Our model uses machines with designs that can provide acceptable results. This study explains a feature type diagnosis of FWT called B-spline with overall accuracy of 94.28%, specificity of 92.30% and sensitivity of 95.45%.

To find the best neighborhood number, the average of all evaluation criteria including sensitivity, specificity, accuracy and F1 score for each table mentioned in the results section was taken horizontally. according to Figure 14, it can be said that the slope of the graph decreases with the increase of k. Table 7 compares the work done by our proposed method with other methods in the past literature. These findings may help resolve a number of problems related to distinguishing covid-19 from non-covid-19. First of all, it has been difficult to obtain empirical evidence of changes in the pneumonic pattern in lung ultrasound images.

Cause of this transform examines the resolution in two time-frequency domains and this transform is superior to similar transforms, it was used in this study. Compared to the similar works shown in Table 7, one of the widely used models for distinguishing covid-19 from non-covid-19 is the CNN network. Deep learning networks require a large number of data for processing and classification, while in this study, by using FBSWT, it was possible to use KNN classifier, which is a simple classifier, on small data and a good result was obtained from proper accuracy. Regarding the extracted features, it can be said that the number of features used in this study is less than other studies. Compared to the wavelet, Fourier, and short-time Fourier transforms, the FWT has one degree of freedom to change the time-frequency resolution, which can weigh the time or frequency domain.

Despite all the advantages of the proposed method, they also have limitations. One of the main challenges in the FWT was that this algorithm had a high computational volume and great complexity, so the B-spline function solved this problem to a large extent. Another limitation when using lung ultrasound data was that the number of subjects was limited, which made it difficult to divide the data into two classes and three classes. Ultrasound images are sensitive to pre-processing because important image information may be lost by incorrect use of the filter. The results of this study show that by using FBSWT, we can hope for the future of using fractional transforms, especially FBSWT in disease diagnosis.

2. Conclusion

Currently, one of the new ways to diagnose infectious lung diseases such as Covid-19 and the degree of involvement is the use of medical images such as lung ultrasound. In this research, lung ultrasound images were used to diagnose the disease of covid-19. Many methods are applied on medical images to make diagnosis faster and with proper accuracy. According to recent papers, researchers have become inclined to use more lung ultrasound images to diagnose covid-19. This research tries to provide solution with appropriate accuracy and speed in the field of time and frequency. In order to extract features for detecting covid-19 from healthy people, FWT of B-spline type, which is a generalization of WT, was used. The main advantage of this method is to use the features in the images in both time and frequency domains. the FBSWT transform method has so far and we were able to show that this method combined with machine learning techniques is suitable for detecting the disease of covid-19 from healthy people, in addition, compared to the WT, the proposed FBSWT method performed about 5% better in accuracy and the results it showed promising results.

Author Statement

Salar Mohammadi: Methodology, Software, Formal Analysis, Writing Original Draft, Review and Editing.

Saeid Rashidi: Supervision, the idea of the research, helping in Programming, Helping in editing paper.

Data availability the database used in this study was downloaded from the GitHub site, that is available by link (https://github.com/jannisborn/covid19_pocus_ultrasound).

Funding: This paper is not sponsored by any person or organization.

Compliance with ethical standards

Research Involving Human Participants and/or Animals This paper does not contain any studies with human participants or animals performed by any of the authors.

Informed Consent Informed consent was obtained from all individual participants included in the study.

Conflict of Interest The authors declare that they have no conflict of interest.

References

1. Yüce, M., E. Filiztekin, and K.G. Özkaya,"COVID-19 diagnosis -A review of current methods", *Biosens Bioelectron*, 172: p. 112752 (2021).
2. Kashiwagi, K., Ishii Y., Aoki K., et al., "Immunochromatographic test for the detection of SARS-CoV-2 in saliva", *J Infect Chemother*, 20:(2)27.21p. 384-386 (2021).
3. Sharma, A., I. Ahmad Farouk, and S. Lal, "COVID-19: A review on the novel coronavirus disease evolution, transmission, detection, control and prevention", *Viruses*; 13: 202 (2021).
4. de Miguel-Yanes JM., Lopez-de-Andres A., Jiménez-Garcia R., et al. "Incidence, outcomes and sex-related disparities in pneumonia: A matched-pair analysis with data from Spanish hospitals",(2016–2019), *Journal of clinical medicine*, 23;10(19):4339 (2021).
5. Cunha BA. "Pneumonia in the elderly", *Clinical microbiology and infection*;1:7(11):581-8 (2001).
6. Picano, E., Scali MC., Ciampi Q., et.al. "Lung Ultrasound for the Cardiologist". *JACC Cardiovasc Imaging*, 11(11): p. 1692-1705 (2018).
7. Smith, MJ., Hayward SA., Innes SM., et al. "Point-of-care lung ultrasound in patients with COVID-19 - a narrative review", *Anaesthesia*,. 75(8): p. 1096-1104 (2020).
8. Hamet, P. and J. Tremblay, "Artificial intelligence in medicine", *Metabolism*, 69s: p. S36-s40 (2017).
9. Kumar V, Singh D, Kaur M, et al. "Overview of current state of research on the application of artificial intelligence techniques for COVID-19", *PeerJ computer science*. 26;7:e564 (2021).
10. Zhang, D., "Wavelet Transform, in Fundamentals of Image Data Mining: Analysis, Features, Classification and Retrieval", D. Zhang, Editor, *Springer International Publishing*: Cham. p. 35-44 (2019).
11. Jin, W., L. Dai., Ge L., et al. "Wavelet Transform Image Enhancement Algorithm-Based Evaluation of Lung Recruitment Effect and Nursing of Acute Respiratory Distress Syndrome by Ultrasound Image", *Journal of Healthcare Engineering*, p. 8960465 (2021).
12. Mendlovic, D., Zalevsky Z., Mas D., et al., "Fractional wavelet transform", *Applied Optics*, 36(20): p. 4801-4806 (1997).
13. Shi, J., N. Zhang, and X. Liu, "A novel fractional wavelet transform and its applications", *Science China Information Sciences*, 55(6): p. 1270-1279 (2012).
14. Muhammad G, Hossain MS., "COVID-19 and non-COVID-19 classification using multi-layers fusion from lung ultrasound images", *Information Fusion*. 1;72:80-8 (2021).
15. Born, J., Brandle G., Cossio M., et al., "POCOVID-Net: automatic detection of COVID-19 from a new lung ultrasound imaging dataset (POCUS)", *arXiv preprint arXiv*:200,4/12084 (2020).
16. Olgers, T.J., Azizi N., Blans MJ., et al., "Point-of-care Ultrasound (PoCUS) for the internist in Acute Medicine: a uniform curriculum", *The Netherlands journal of medicine*, 77(5): p. 168-176 (2019).
17. Shi, J., Zhao Y., Xiang W., et al. "Deep Scattering Network With Fractional Wavelet Transform", *IEEE Transactions on Signal Processing*, 69: p. 4740-4757 (2021).
18. Diaz- scobar J, Ordóñez-Guillén NE, Villarreal-Reyes S, et al. "Deep-learning based detection of COVID-19 using lung ultrasound imagery", *Plos one*. 13;16(8): e0255886 (2021).
19. Ebadi SE, Krishnaswamy D, Bolouri SE, et al. "Automated detection of pneumonia in lung ultrasound using deep video classification for COVID-19", *Informatics in Medicine Unlocked*. 25:100687 (2021).
20. Baum ZMC, Bonmati E, Cristoni L., et al. "Image quality assessment for closed-loop computer-assisted lung", *SPIE Digital Library* Vol. 11598, pp. 183-189 (2021).
21. Awasthi N., Dayal A., Cenkeramaddi LR., et al. "Mini-COVIDNet: efficient lightweight deep neural network for ultrasound based point-of-care detection of COVID-19", *IEEE Transactions on Ultrasonics, Ferroelectrics, and Frequency Control*. 68(6):2023-37 (2021).
22. Born, J., Wiedemann., Cossio., et al., "Accelerating Detection of Lung Pathologies with Explainable Ultrasound Image Analysis", *Applied Sciences*,11(2): p. 672 (2021).
23. Balocco, S., Gatta C., Ferre JM., et al., "Ultrasound Despeckle Methods, in Ultrasound Imaging: Advances and Applications", J.M. Sanches, A.F. Laine, and J.S. Suri, Editors, *Springer US*: *Boston, MA*. p. 49-71 (2012).

24. Djurović, I., "BM3D filter in salt-and-pepper noise removal", *EURASIP Journal on Image and Video Processing*. vol (1): p. 13 (2016).
25. Zhang, J., Xiong R., Zhao C., et al., "CONCOLOR: Constrained non-convex low-rank model for image deblocking", *IEEE Transactions on Image Processing*,. 25(3): p. 1246-1259 (2016).
26. Yahya, A.A., Tan J., Su B., et al., "BM3D image denoising algorithm based on an adaptive filtering", *Multimedia Tools and Applications*, 79(27): p. 20391-20427 (2020).
27. Barki, Z., Seddik CBJ., and Seddik H., "Building a modified block matching kernel based on Wave Atom transform for efficient image denoising", *The Egyptian Journal of Remote Sensing and Space Science*, 24(3, Part 2): p. 857-878 (2021).
28. Mostafa, A., Barghash TO., Assaf AAS., et al. "Multi-sensor Gait Analysis for Gender Recognition", *in ICINCO*, (2020).
29. Blu T, Unser M. "The fractional spline wavelet transform: definition end implementation", I*n IEEE International Conference on Acoustics, Speech, and Signal Processing*. (Cat. No. 00CH37100). Vol. 1, pp. 512-515 (2000).
30. Roberts J, Tsiligkaridis T. "Ultrasound diagnosis of COVID-19: robustness and explain ability", *arXiv preprint arXiv*:2012.01145 (2020).
31. Roy, S., Menapace, W., Oei, S., et al. A. "Deep learning for classification and localization of COVID-19 markers in point-of-care lung ultrasound", *IEEE Trans. Med. Imaging*, 39, 2676–2687 (2020).
32. Liu L, Lei W, Wan X, et al. " Semi-supervised active learning for COVID-19 lung ultrasound multi-symptom classification", *In 2020 IEEE 32nd International Conference on Tools with Artificial Intelligence (ICTAI)*. pp 1268-1273 (2020).
33. Barros B, Lacerda P, Albuquerque C, et al. "Pulmonary COVID-19: Learning spatiotemporal features combining cnn and lstm networks for lung ultrasound video classification", *Sensors*. 14;21(16):5486 (2021).
34. Arntfield R, VanBerlo B, Alaifan T, et al. "Development of a convolutional neural network to differentiate among the etiology of similar appearing pathological B lines on lung ultrasound: a deep learning study", *BMJ open*. 1;11(3): e045120 (2021).

Saeid Rashidi was born in Tehran, Iran, in 1973. He received the Ph.D. degree in biomedical engineering from the Amirkabir University of Technology, Tehran, Iran, in 2013. Currently, he is an assistant professor in Medical Sciences and Technologies Faculty, Science and Research Branch, Islamic Azad University. His research activities are concentrated in the area of biomedical signal and image processing, biometric, motor control and chaos.

Salar Mohammadi was born in Tehran, Iran, in 1997. He received a bachelor's degree in medical engineering from the Islamic Azad University of Tehran, branch of medical sciences, in 2019. He is a graduate of medical engineering majoring in bioelectric from the Faculty of Medical Sciences and Technologies, Islamic Azad University, Science and Research branch. His research activities are concentrated in the area of biomedical signal, image processing and machine learning.

LIST OF FIGURES CAPTIONS:

LIST OF TABLES CAPTIONS:

LIST OF FIGURES:

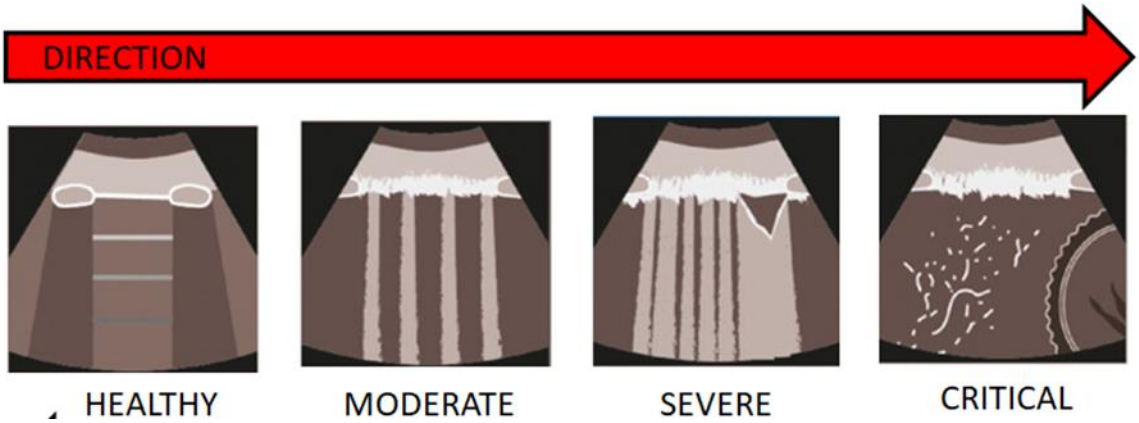

Figure 1.

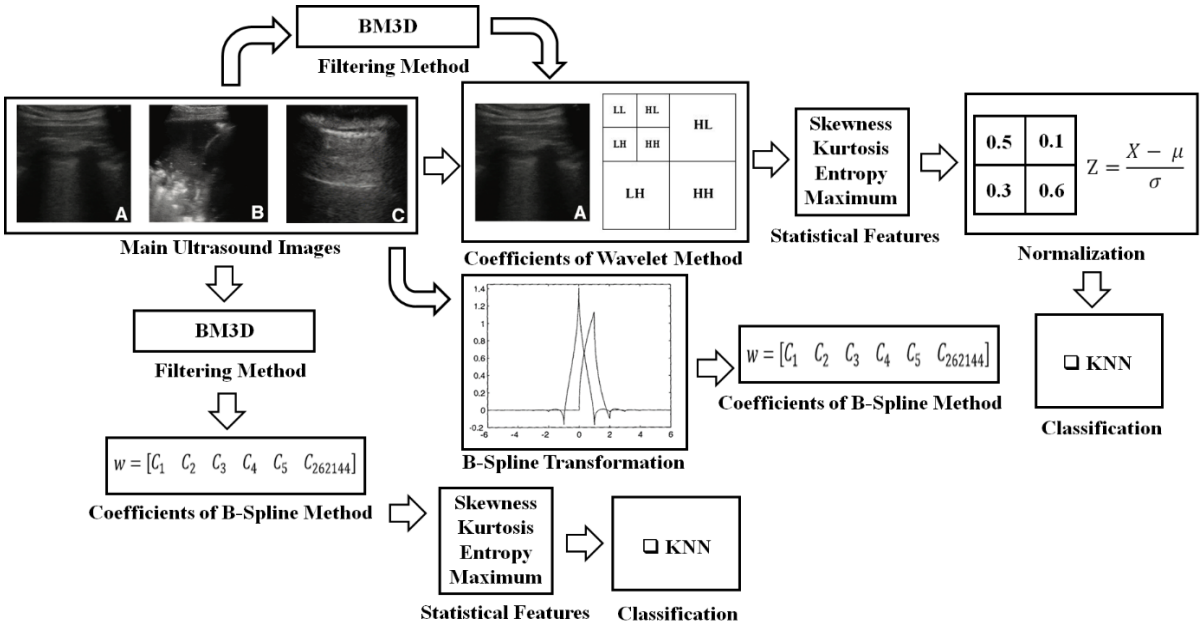

Figure 2.

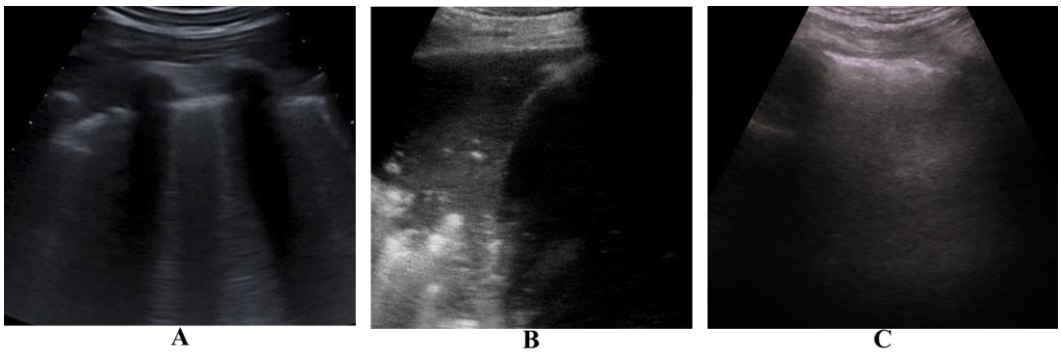

Figure 3.

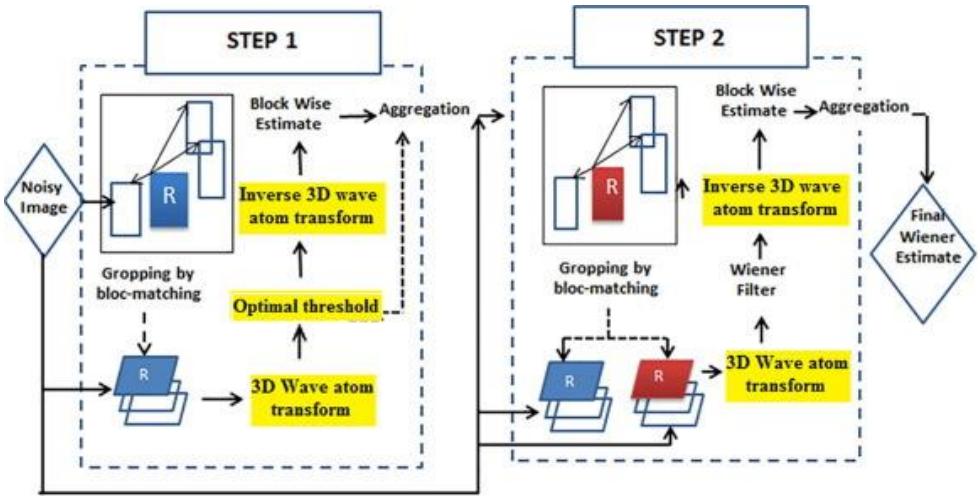

Figure 4.

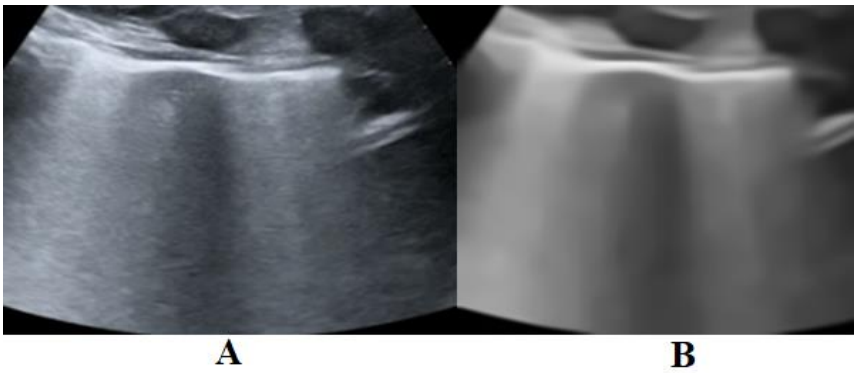

Figure 5.

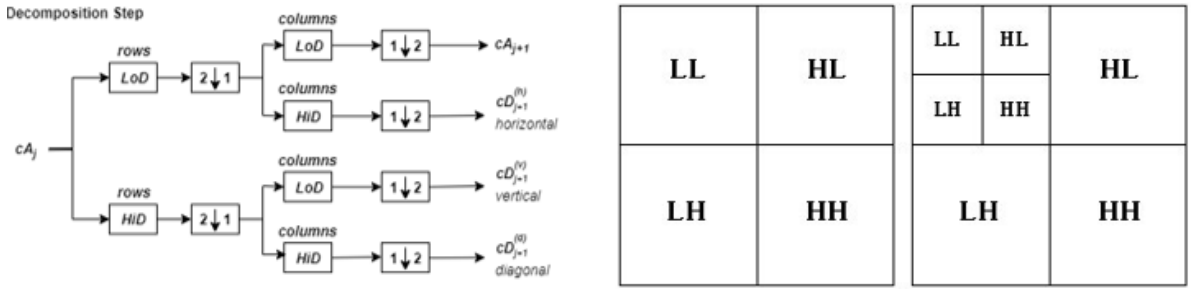

Figure 6.

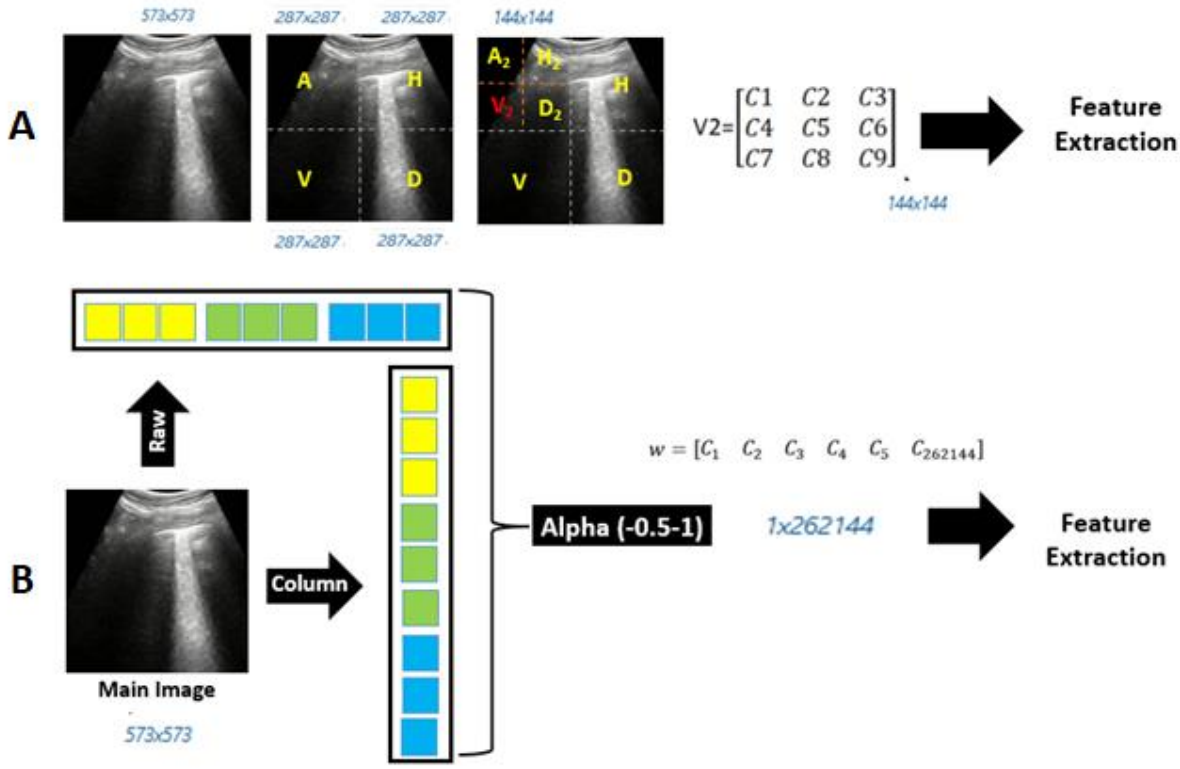

Figure 7.

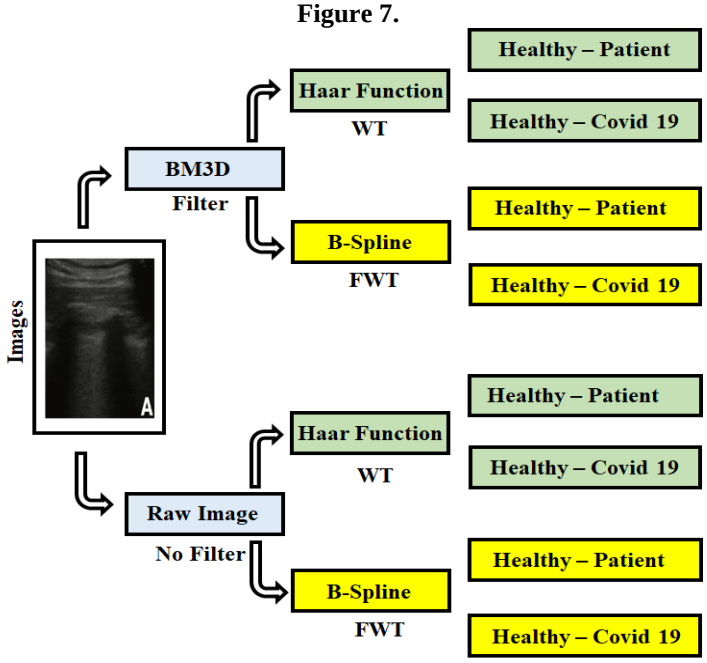

Figure 8.

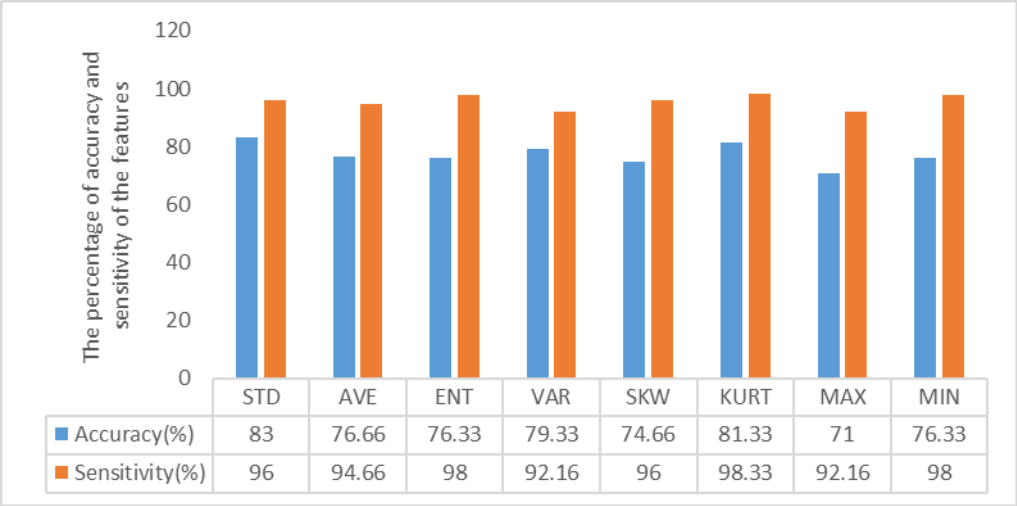

	STD	AVE	ENT	VAR	SKW	KURT	MAX	MIN
Accuracy(%)	83	76.66	76.33	79.33	74.66	81.33	71	76.33
Sensitivity(%)	96	94.66	98	92.16	96	98.33	92.16	98

Figure 9.

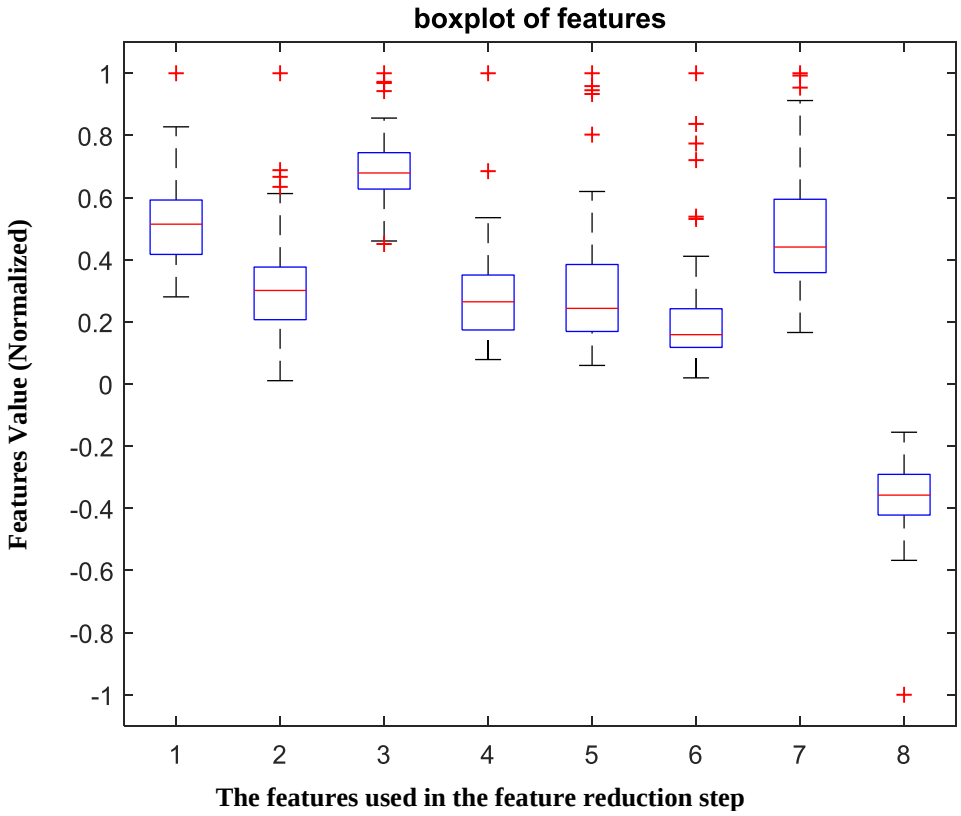

Figure 10.

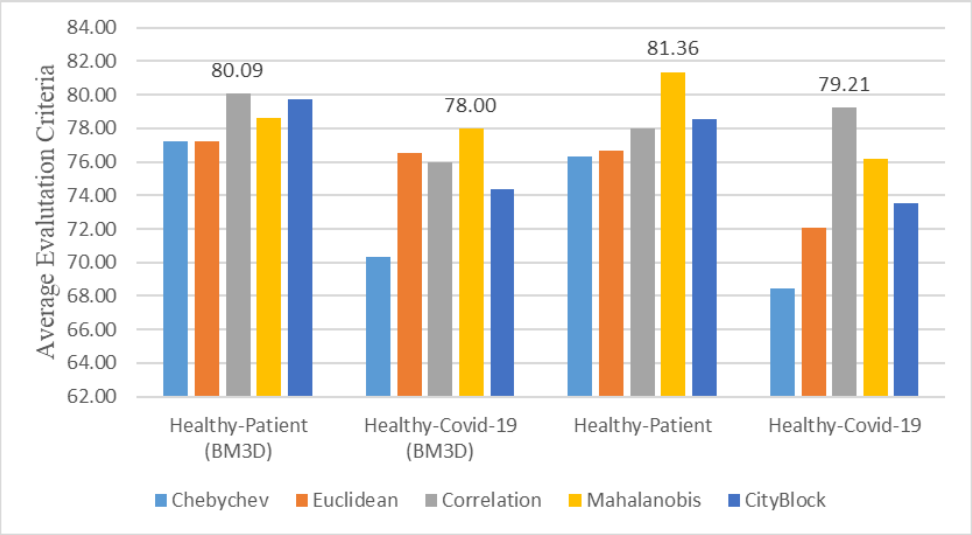

Figure 11.

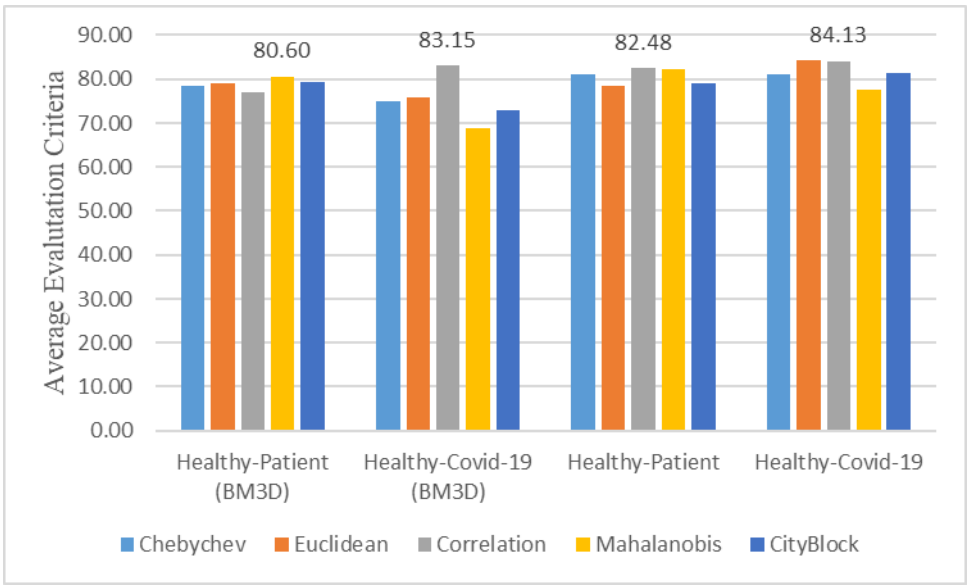

Figure 12.

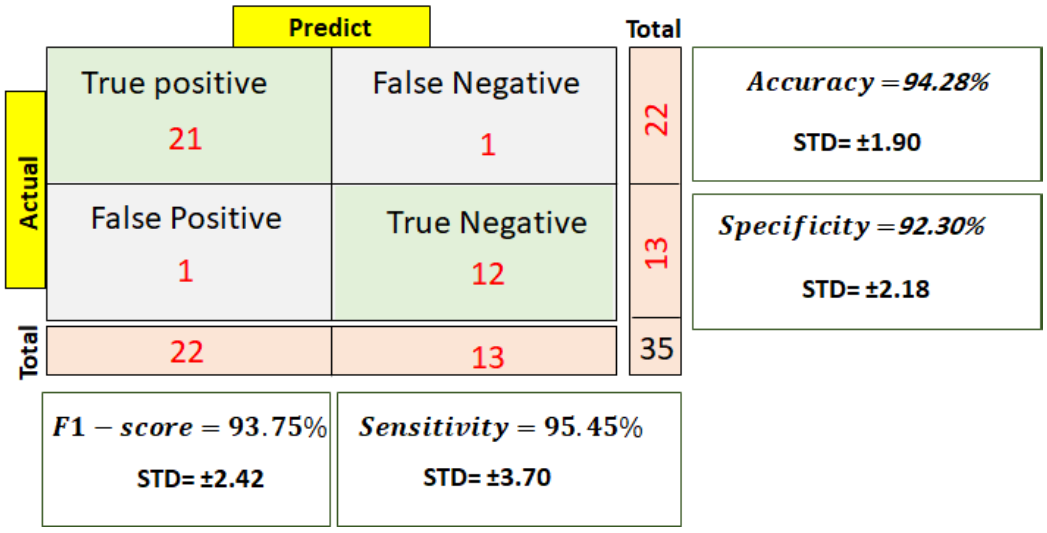

Figure 13.

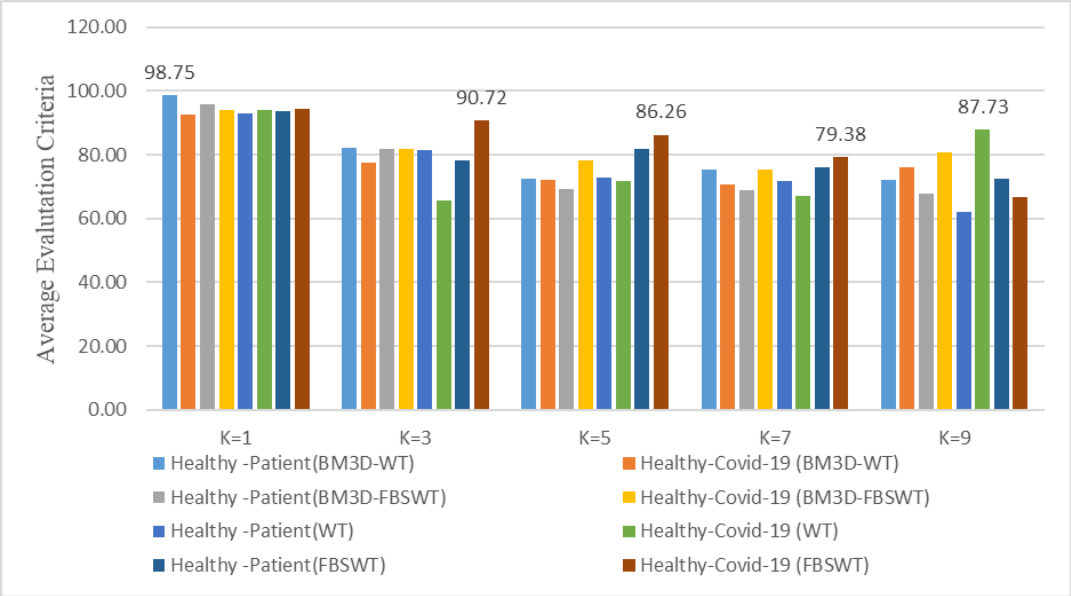

Figure 14.

LIST OF TABLES:

Table 1.

Images	Convex		Linear		
	Vid	Img	Vid	Img	Sum
Covid	40	16	4	3	63
BP	23	7	2	2	34
VP	3	-	4	-	7
Healthy	20	5	10	-	35
Sum	86	28	20	5	139

Table 2.

BM3D FILTER				
K	Sensitivity(%)	Specificity(%)	Accuracy (%)	F1-Score(%)
K=1	97.82	100	98.30	98.90
K=3	92.63	61.53	84.74	90.32
K=5	91.30	33.48	77.96	86.59
K=7	97.82	30.76	83.05	90.00
K=9	93.55	22.38	81.35	91.03
WITHOUT FILTER				
K=1	93.82	90.74	91.61	95.10
K=3	91.52	53.84	88.13	92.78
K=5	87.40	30.76	83.05	90.00
K=7	84.07	30.76	81.74	91.08
K=9	79.36	7.69	74.66	86.46

Table 3.

BM3D FILTER				
K	Sensitivity(%)	Specificity(%)	Accuracy (%)	F1-Score(%)
K=1	90.90	92.30	91.42	95.23
K=3	81.81	69.23	77.14	81.81
K=5	72.64	68.44	71.42	76.19
K=7	80.07	53.81	70.68	78.26
K=9	79.64	64.70	77.56	82.66
WITHOUT FILTER				
K=1	95.45	92.30	94.28	93.61
K=3	77.27	46.15	65.71	73.91
K=5	93.14	38.46	74.28	81.35
K=7	90.90	30.76	68.57	78.43
K=9	88.61	92.30	89.28	80.74

Table 4.

BM3D FILTER				
K	Sensitivity(%)	Specificity(%)	Accuracy (%)	F1-Score(%)
K=1	97.82	92.30	96.61	96.42
K=3	91.30	61.53	84.74	90.32
K=5	91.30	23.07	76.27	85.71
K=7	95.65	15.38	77.96	87.12
K=9	93.47	15.38	76.27	86.00
WITHOUT FILTER				
K=1	94.82	92.30	93.61	93.57
K=3	93.47	46.15	83.05	89.58
K=5	95.65	53.84	86.44	91.66
K=7	93.65	38.46	83.05	89.79
K=9	91.47	30.76	79.66	87.75

Table 5.

BM3D FILTER				
K	Sensitivity(%)	Specificity(%)	Accuracy (%)	F1-Score(%)
K=1	95.45	92.30	94.28	93.75
K=3	79.47	84.61	80.00	82.92
K=5	77.27	76.92	77.14	80.95
K=7	72.72	76.92	74.28	78.04
K=9	81.81	76.92	80.00	83.72
WITHOUT FILTER				
K=1	95.45	92.30	94.28	95.45
K=3	93.53	84.61	91.42	93.33
K=5	86.36	84.61	85.71	88.37
K=7	90.90	61.53	80.00	85.10
K=9	68.18	61.53	65.71	71.42

Table 6.

Method	Filter	Classes	Acc (%)	Sen (%)	Spe (%)	F1
WT	BM3D	Healthy - Patient	97.82	100.00	98.30	98.90
	BM3D	Healthy-Covid-19	90.90	92.30	91.42	95.23
	-	Healthy - Patient	93.28	90.74	91.58	95.10
	-	Healthy-Covid-19	95.15	92.30	94.28	93.61
FBSWT	BM3D	Healthy - Patient	97.82	92.71	96.61	96.42
	BM3D	Healthy-Covid-19	95.45	93.30	94.28	93.75
	-	Healthy - Patient	94.82	92.30	93.65	93.57
	-	Healthy-Covid-19	95.45	92.30	94.28	95.45

Table 7.

Author's	Method	Database	Class	Sen (%)	Spe (%)	Acc (%)
Born et. al [15].	Frame Base	POCUS	Healthy, Covid-19 and Pneumonia	90.00	96.00	-
Roberts et. al [30].	CNN-(ERM)	POCUS	Healthy, Covid-19 and Pneumonia	-	-	85.99
Roy et. al [31].	Spatial Transformer Networks	ICLUS-DB	Sever of covid-19	-	-	96.00
Liu et. al[32].	ResNet50	ICLUS-DB	A line and B line	99.00	92.00	98.00
Barros et. al [33].	CNN	POCUS	Healthy, Covid-19 and Pneumonia	97.00	-	93.00
Baum et al [20].	quality assessment method	Butterfly, Guilford	Site A and Site B	91.00	97.00	95.00
Arntfield et al [34].	Xception	ICLUS-DB	Covid-19 and Non Covid-19	92.00	88.00	-
Ebadi et.al [19].	Kinetics-ID3	POCUS	Site A and Site B	-	-	90.00
Diaz-Escobar [18].	Inception V3	POCUS	Covid-19, non Covid-19	-	-	91.50
Muhammad et. al[14].	CNN	POCUS	COVID-19 and Non-COVID-19	-	-	91.80
Purpose Method	**WT**	**POCUS**	**Healthy and Covid-19**	**90.90**	**92.30**	**91.42**
	FBSWT		**Healthy and Covid-19**	**95.45**	**93.30**	**94.28**